



**HAL**  
open science

## Barium complexes with crown-ether-functionalised amidinate and iminoanilide ligands for the hydrophosphination of vinylarenes

Erwann Le Coz, Hanieh Roueindeji, Thierry Roisnel, Vincent Dorcet, Jean-François Carpentier, Yann Sarazin

### ► To cite this version:

Erwann Le Coz, Hanieh Roueindeji, Thierry Roisnel, Vincent Dorcet, Jean-François Carpentier, et al. Barium complexes with crown-ether-functionalised amidinate and iminoanilide ligands for the hydrophosphination of vinylarenes. Dalton Transactions, 2019, 48 (25), pp.9173-9180. 10.1039/c9dt01512d . hal-02150460

**HAL Id: hal-02150460**

**<https://univ-rennes.hal.science/hal-02150460>**

Submitted on 8 Jul 2019

**HAL** is a multi-disciplinary open access archive for the deposit and dissemination of scientific research documents, whether they are published or not. The documents may come from teaching and research institutions in France or abroad, or from public or private research centers.

L'archive ouverte pluridisciplinaire **HAL**, est destinée au dépôt et à la diffusion de documents scientifiques de niveau recherche, publiés ou non, émanant des établissements d'enseignement et de recherche français ou étrangers, des laboratoires publics ou privés.

**Barium complexes with crown-ether-functionalised amidinate and iminoanilide ligands  
for the hydrophosphination of vinylarenes†**

*(a contribution to the special issue of Dalton Transactions dedicated to nitrogen-based ligands)*

Erwann Le Coz,<sup>‡</sup> Hanieh Roueindeji,<sup>‡</sup> Thierry Roisnel, Vincent Dorcet,  
Jean-François Carpentier and Yann Sarazin\*

Univ Rennes, CNRS, ISCR (Institut des Sciences Chimiques de Rennes) – UMR 6226, F-35000 Rennes,  
France.

Corresponding author: [yann.sarazin@univ-rennes1.fr](mailto:yann.sarazin@univ-rennes1.fr)

† Electronic supplementary information (ESI) available: full experimental details including NMR spectra  
and crystallographic data for CCDC 1896037-1896039 and 1897231.

## Abstract

The detailed multistep syntheses of two nitrogen-based sterically congested iminoanilidine and amidine proligands bearing a tethered 15-member aza-ether-crown macrocycle, namely  $\{I^A^{crown}\}H$  and  $\{Am^{crown}\}H$ , are reported. These proligands react with  $[Ba\{N(SiMe_2H)_2\}_2 \cdot (thf)_n]$  to generate the heteroleptic barium complexes  $[\{I^A^{crown}\}BaN(SiMe_2H)_2]$  (**5**) and  $[\{Am^{crown}\}BaN(SiMe_2H)_2]$  (**6**) in high yields. These complexes exhibit high coordination numbers (resp. eight and seven), and are in addition stabilised by mild  $Ba \cdots H-Si$  interactions. Unusually for oxophilic elements such as barium, the amidinate ligand in **6** is only  $\eta^1$ -coordinated. Complexes **5** and **6** mediate the intermolecular hydrophosphination of styrene with primary ( $PhPH_2$ ) and secondary ( $HPPH_2$ ) phosphines. Their catalytic performance compares favourably with those of other barium precatalysts for these reactions. During the course of the hydrophosphination of styrene with  $HPPH_2$  catalysed by **5**, the phosphide complex  $[\{I^A^{crown}\}BaPPh_2]$  (**7**) could be intercepted and crystallographically characterised.

## Introduction

The past 15 years have experienced the emergence of main group metals molecular (pre)catalysts built on abundant metals as suitable alternatives to mainstream homogenous catalytic systems devised around late transition metals. Amongst these, the three large alkaline earths (= Ae) calcium, strontium and barium have been used to a great effect to fabricate a range of potent catalysts.<sup>1</sup> Following the seminal works by the groups of Hill and Harder, Ca, Sr and Ba complexes have been used to catalyse C–N bond formation in the intramolecular<sup>2</sup> and intermolecular<sup>3</sup> hydroamination of alkenes. Effective alkene hydrosilylation mediated by Ae complexes has been known for 10 years.<sup>4</sup> By comparison, Ae-promoted regioselective C–P (alkene<sup>5</sup> and alkyne<sup>6</sup> hydrophosphination) and N–Si (amine/hydrosilanes heterodehydrocouplings<sup>7</sup>) bond creations are recent addition to the arsenal of tools implementable by synthetic chemists.

Organophosphorus compounds find widespread applications, e.g. as ligands in coordination chemistry and for metal-catalysed organic transformations,<sup>8</sup> in industry as pest control and pesticides, and also owing to their biological activity, e.g. such as antibiotics and antitumor agents.<sup>9</sup> The 100% atom-efficient catalysed addition of H–P bonds across unsaturated C=C bonds is an attractive way to produce a variety of C–P bonds. Across an homologous series of complexes of large Ae metals, barium alkene hydrophosphination precatalysts have displayed the most impressive performances, enabling addition of secondary phosphines across activated alkenes (vinylarenes, conjugated dienes) with high anti-Markovnikov regioselectivity and reaction rates.<sup>3c,3d</sup> It was found that reaction rates increase upon descending group according to Ca < Sr < Ba, a trend repeated on many occasions of Ae-catalysed reactions,<sup>3-7,10</sup> albeit not systematically.<sup>2,7a,11</sup>

The design of bulky, monoanionic ligand (= {Lig}<sup>−</sup>) capable of sheltering the large, electropositive and polarisable Ae<sup>2+</sup> ions ( $r_{\text{ionic}}$ : Ca<sup>2+</sup>, 1.00 Å; Sr<sup>2+</sup>, 1.18 Å; Ba<sup>2+</sup>, 1.35 Å) has been key to the implementation of Ae-mediated catalysis. In particular, heteroleptic precatalysts of the type {Lig}AeX (where X<sup>−</sup> = N(SiMe<sub>2</sub>H)<sub>2</sub><sup>−</sup>, N(SiMe<sub>3</sub>)<sub>2</sub><sup>−</sup>, CH(SiMe<sub>3</sub>)<sub>2</sub><sup>−</sup>, PPh<sub>2</sub><sup>−</sup>, etc.) provide on the whole the best versatility and turnovers.<sup>1</sup> In this context, nitrogen-based ligands have had the upper hand.<sup>1,12</sup> Most prominently, the β-diketiminate {BDI<sup>Dipp2</sup>}<sup>−</sup> (where BDI<sup>Dipp2</sup> = CH[C(CH<sub>3</sub>)NDipp]<sub>2</sub>, Dipp = 2,6-diisopropylphenyl, Figure 1) has been most useful, affording access to unusual or highly reactive low coordinate Ae species such as the ubiquitous [{BDI<sup>Dipp2</sup>}CaN(SiMe<sub>3</sub>)<sub>2</sub>.(thf)] (**1**) and its derivatives with smaller X<sup>−</sup> functionalities.<sup>1-7,13</sup> Related [{I<sup>A</sup><sup>Dipp2</sup>}AeX.(thf)<sub>n</sub>] complexes (X<sup>−</sup> = N(SiMe<sub>3</sub>)<sub>2</sub><sup>−</sup> or CH(SiMe<sub>3</sub>)<sub>2</sub><sup>−</sup>, n = 1-2 Figure 1) incorporating the hindered iminoanilide {I<sup>A</sup><sup>Dipp2</sup>}<sup>−</sup> are excellent hydroamination and hydrophosphination precatalysts, especially for Ae = Ba (**2**).<sup>3c,3d</sup> Besides, amidinates have been shown to constitute suitable ligand platforms for the synthesis of original heteroleptic Ae complexes, e.g. molecular hydrides as in **3**.<sup>14</sup> Elsewhere, the utilisation of multidentate neutral (co)ligands such as polyamines and aza-crown-ethers has also yielded very active Ae hydrides hydrogenation catalysts<sup>4b,15</sup> and various Ae polymerisation catalysts, e.g. [{LO<sup>NO4</sup>}BaN(SiMe<sub>2</sub>H)<sub>2</sub>] (**4**) bearing the multidentate aza-crown-ether-phenolate {LO<sup>NO4</sup>}<sup>−</sup>.<sup>10a,16</sup>

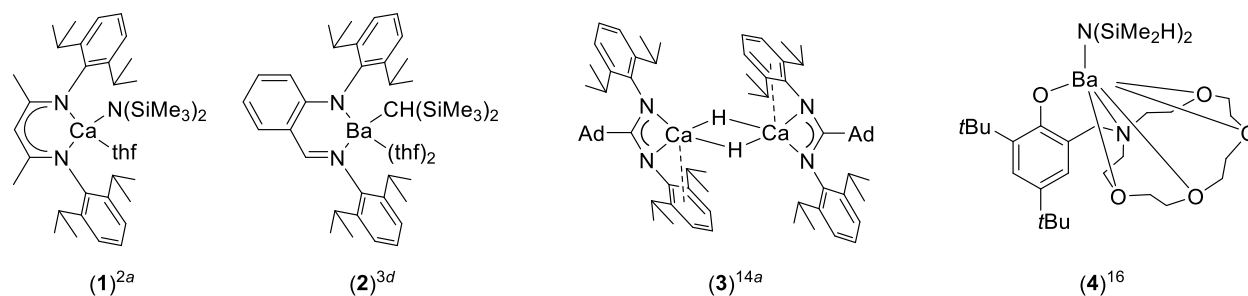


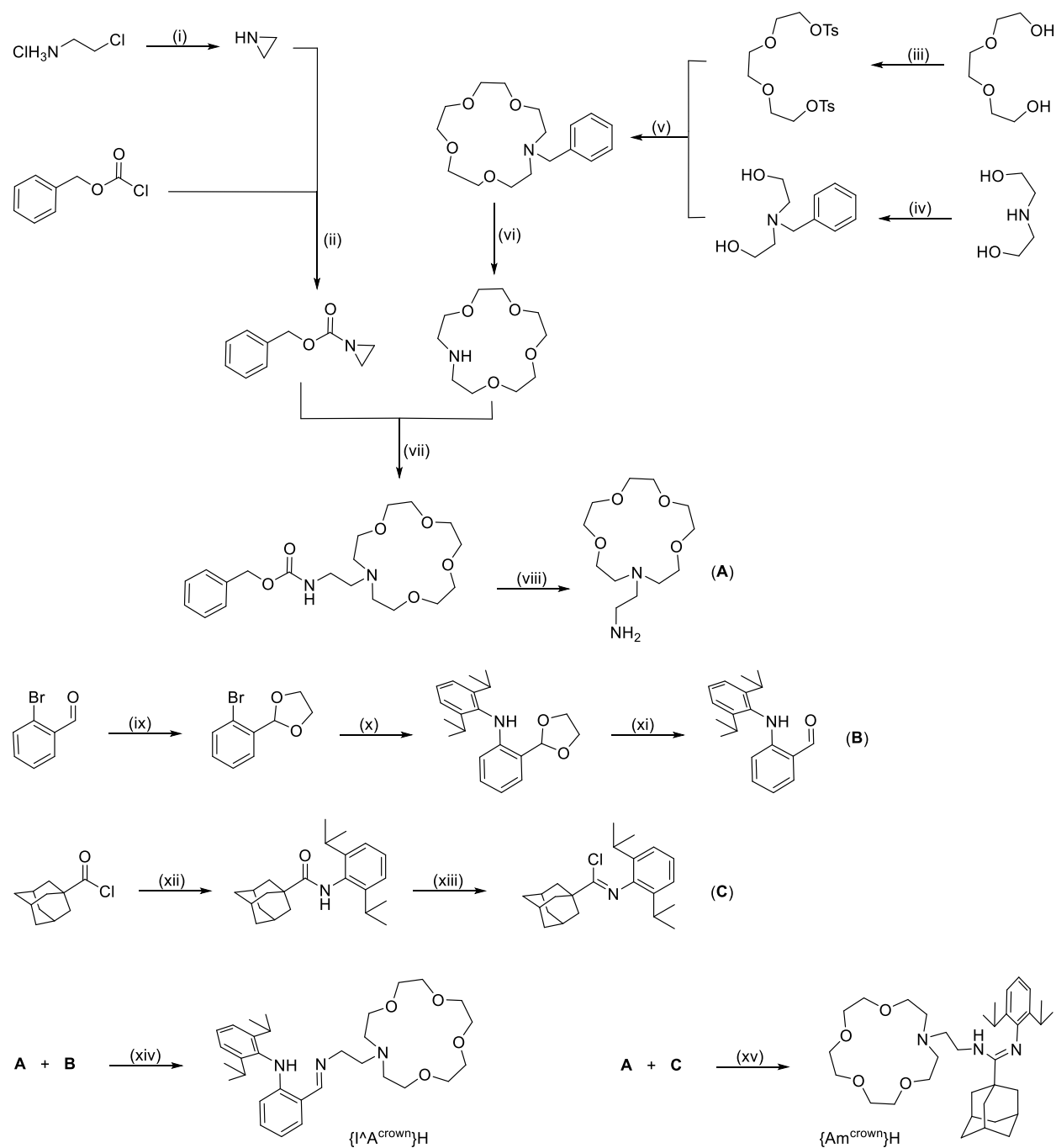
**Fig. 1** Examples of *N*-based and macrocycle-functionalised alkaline earth molecular complexes. Ad = adamantyl.

As part of our ongoing studies in the area of Ae-mediated molecular catalysis, we thought of combining the advantages of *N*-based ligands and macrocycles into ligand frameworks able to stabilise barium species. We report here on the design of new bulky iminoaniline and amidine proligands that include a tethered macrocycle. We anticipated that the pairing of bulky iminoanilide or amidinate, which have shown their ability to kinetically stabilise Ae complexes against ligand scrambling, with a macrocycle known for its ability to stabilise otherwise electronically unsaturated Ae species, would deliver original ligands particularly well suited to this chemistry. These ligands were used to generate heteroleptic barium amido complexes that in turn display good performance in the hydrophosphination of vinylarenes. Synthetic, structural and catalytic features of these barium compounds are discussed.

## Results and Discussion

### *Synthesis and characterisation*

The functionalised iminoaniline {I<sup>^A</sup><sup>crow</sup>n}H and amidine {Am<sup>crow</sup>n}H proligands containing a tethered 15-member macrocycle were constructed in convergent multistep syntheses (Scheme 1) that started with the large scale synthesis of 2-(1-aza-15-crown-5)-ethan-1-amine (**A**). Condensation of **A** with the Dipp-*N*-substituted benzaldehyde **B** afforded {I<sup>^A</sup><sup>crow</sup>n}H, whereas {Am<sup>crow</sup>n}H was obtained by reacting **A** with the adamantyl-substituted *N*-Dipp-carbimidoyl chloride **C**. Complete experimental details for the synthesis of the two proligands and of the synthetic intermediates, together with pertaining analytical data, are provided in the Supporting Information.<sup>#</sup> Note that the condensation affording {I<sup>^A</sup><sup>crow</sup>n}H, aka step (xiv) in Scheme 1, requires several days and addition of amine **A** in several portions. Under optimised conditions, this proligand was ultimately obtained in high yield as an off-white oil which solidified slowly upon standing at room temperature. However, we found that the final yields of isolated product could vary to noticeable extents depending on reaction times and protocol for the addition of **A**.



**Scheme 1.** Synthesis of the proligands  $\{I^A{}^{\text{crown}}\}\text{H}$  and  $\{\text{Am}^{\text{crown}}\}\text{H}$ . Reaction conditions: (i) NaOH,  $\text{H}_2\text{O}$ ,  $50\text{ }^\circ\text{C}$ , 4 h, 75%; (ii)  $\text{Et}_2\text{O}$ ,  $\text{NEt}_3$ , 0 to  $20\text{ }^\circ\text{C}$ , 12 h, 51%; (iii) TsCl, DMAP,  $\text{NEt}_3$ ,  $\text{CH}_2\text{Cl}_2$ , 0 to  $20\text{ }^\circ\text{C}$ , 12 h, 85%; (iv)  $\text{BnBr}$ ,  $\text{Na}_2\text{CO}_3$ , acetone, reflux, 4 h, 80%; (v) NaOH,  $n\text{Bu}_4\text{NBr}$ , toluene,  $70\text{ }^\circ\text{C}$ , 10 h, 82%; (vi)  $\text{H}_2$ , Pd/C, MeOH,  $20\text{ }^\circ\text{C}$ , 12 h, 80%; (vii)  $\text{CH}_3\text{CN}/\text{toluene}$  (1:1 v/v), reflux, 24 h, 70%; (viii)  $\text{H}_2$ , Pd/C, MeOH,  $20\text{ }^\circ\text{C}$ , 15 h, 97%; (ix)  $\text{HOCH}_2\text{CH}_2\text{OH}$ , PTSA, toluene, reflux, 48 h, 61%; (x) 2,6-*i*-Pr<sub>2</sub>C<sub>6</sub>H<sub>3</sub>NH<sub>2</sub>, Pd(OAc)<sub>2</sub>, *t*BuOK, *t*Bu<sub>3</sub>, thf, reflux, 16 h; (xi)  $\text{CF}_3\text{COOH}$ , MeOH, 1 h,  $20\text{ }^\circ\text{C}$ , 38%; (xii) 2,6-*i*-Pr<sub>2</sub>C<sub>6</sub>H<sub>3</sub>NH<sub>2</sub>, toluene,  $\text{NEt}_3$ ,  $70\text{ }^\circ\text{C}$ , 3 h, 98%; (xiii)  $\text{SOCl}_2$ , reflux, 3 h, 90%; (xiv) petroleum ether, reflux, 10 d, 90%; (xv)  $\text{NEt}_3$ ,  $\text{CH}_2\text{Cl}_2$ ,  $20\text{ }^\circ\text{C}$ , 72 h, 32%.

The sterically congested amidine  $\{\text{Am}^{\text{crown}}\}\text{H}$  was isolated as analytically pure pale yellow crystals in non-optimised ca. 30% yield by reaction of compounds **A** and **C** under mild and straightforward operating conditions (see Scheme 1). Alternatively, it was obtained in 70-80% yield as an oily material, although NMR analysis showed in these cases the presence of trace amounts of residual impurities. Both proligands were fully characterised by NMR, mass spectrometry and combustion analyses. They are highly soluble in all common organic solvents, including aliphatic hydrocarbons. Single crystals of  $\{\text{I}^{\wedge}\text{A}^{\text{crown}}\}\text{H}$  suitable for X-ray diffraction crystallography were grown from the oily material upon standing at room temperature. Its molecular solid-state structure, with notable interatomic distances, are given in Figure 2. Crystals of  $\{\text{Am}^{\text{crown}}\}\text{H}$  were also analysed, but the final refinement of the structure was high (>20%) due to high disorder.

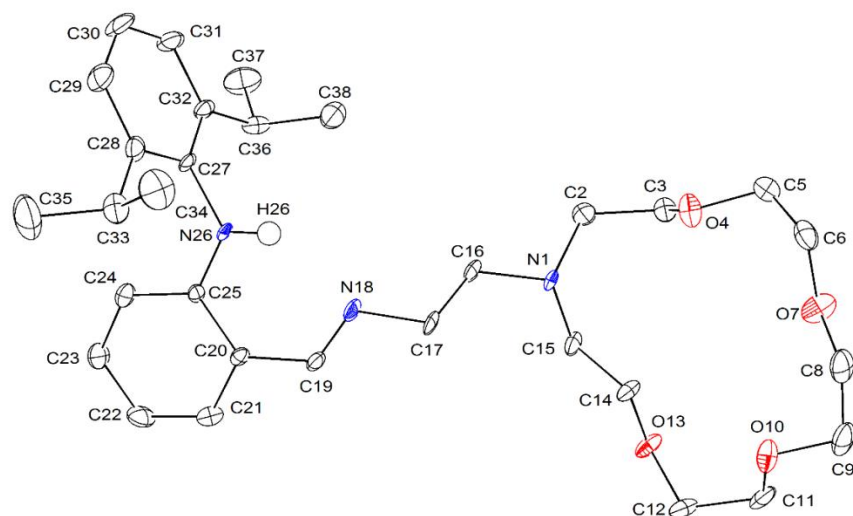
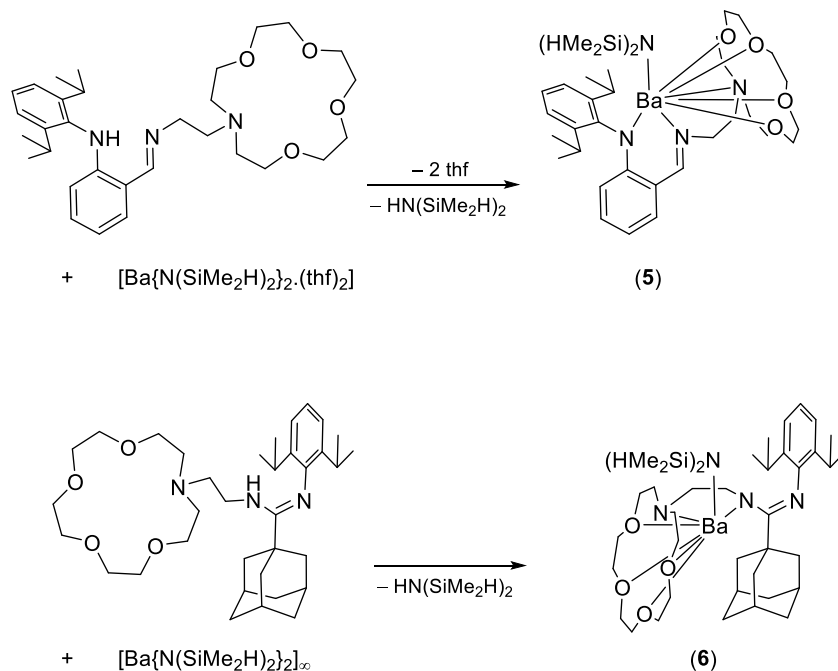


**Fig. 2.** ORTEP representation of the molecular solid-state structure of  $\{\text{I}^{\wedge}\text{A}^{\text{crown}}\}\text{H}$ . Ellipsoids at the 50% probability level. Only one of the two identical molecules in the asymmetric unit is depicted. *CH* atoms omitted for clarity. Selected interatomic distances (Å): C17-N18 = 1.461(4), N18-C19 = 1.268(4), N1-C16 = 1.458(3), N1-C15 = 1.469(4), N1-C2 = 1.470(4), C25-N26 = 1.369(4), N26-C27 = 1.428(4).

The amido group  $\text{N}(\text{SiMe}_2\text{H})_2^-$  has been introduced in barium chemistry as a useful tool for the stabilisation of barium complexes through the presence of intramolecular  $\text{Ba}\cdots\text{H}-\text{Si}$  anagostic interactions, as in a monometallic aminoether-phenolato complex  $[\{\text{LO}^{\text{NO}_4}\}\text{BaN}(\text{SiMe}_2\text{H})_2]$  (**3**)<sup>16</sup> or in the trinuclear cluster  $[\text{Ba}_3\{\text{OSi}(\text{O}t\text{Bu})_3\}_3\{\text{N}(\text{SiHMe}_2)_2\}_3]$ .<sup>17</sup> Following the same line, the stoichiometric reaction of  $[\text{Ba}\{\text{N}(\text{SiMe}_2\text{H})_2\}_2\cdot(\text{thf})_2]$  with the iminoaniline  $\{\text{I}^{\wedge}\text{A}^{\text{crown}}\}\text{H}$  returned, upon selective release of one equivalent of  $\text{HN}(\text{SiMe}_2\text{H})_2$ , the heteroleptic complex  $[\{\text{I}^{\wedge}\text{A}^{\text{crown}}\}\text{BaN}(\text{SiMe}_2\text{H})_2]$  (**5**) as an orange solid in

86% yield (Scheme 2). The  $^1\text{H}$  NMR spectrum of **5** in  $\text{thf-}d_8$  is characterised by a singlet at  $\delta$  8.04 ppm for the  $\text{CH}=\text{N}$  imine hydrogen, and a multiplet at  $\delta$  4.57 ppm for the  $\text{SiH}$  hydrogen. There is a substantial level of fluxionality in the complex, as the resonances for  $\text{OCH}_2$ ,  $\text{CH}(\text{CH}_3)_2$  and  $\text{Si}(\text{CH}_3)_2$  moieties are somewhat broad at room temperature. Similarly, the amidinate complex  $[\{\text{Am}^{\text{crown}}\}\text{BaN}(\text{SiMe}_2\text{H})_2]$  (**6**) was isolated as colourless microcrystals in 85% yield following treatment of  $[\text{Ba}\{\text{N}(\text{SiMe}_2\text{H})_2\}_2]_\infty$  with one equivalent of  $\{\text{Am}^{\text{crown}}\}\text{H}$  and release of  $\text{HN}(\text{SiMe}_2\text{H})_2$ . Complexes **5** and **6** are sparingly to moderately soluble in hydrocarbons (petroleum ether, benzene and toluene), and dissolve well in ethers. The presence of two stretching bands for  $\text{Si-H}$  bonds at  $2052$  and  $1990\text{ cm}^{-1}$  (for **5**) and at  $2014$  and  $1975\text{ cm}^{-1}$  (for **6**) in the FTIR spectra of the two complexes recorded as Nujol mulls is consistent with  $\text{Ba}\cdots\text{H-Si}$  anagostic interactions in the solid state. This is corroborated by the  $^1\text{H}$  NMR spectrum of **6** recorded in  $\text{thf-}d_8$ , where the  $^1J_{\text{SiH}}$  coupling constant of  $160\text{ Hz}$  is also diagnostic of mild  $\text{Ba}\cdots\text{H-Si}$  interactions in solution.



**Scheme 2.** Syntheses of  $[\{\text{I}^{\text{A}^{\text{crown}}}\}\text{BaN}(\text{SiMe}_2\text{H})_2]$  (**5**),  $[\{\text{Am}^{\text{crown}}\}\text{BaN}(\text{SiMe}_2\text{H})_2]$  (**6**).

The molecular solid-state structure of **5** depicted in Figure 3 shows the complex to rest in an eight-coordinate environment, with coordination of all heteroatoms on the ancillary ligand onto the metal centre completed by the  $\text{N}_{\text{silazide}}$  atom from the tetramethyldisilazide co-ligand. The  $\text{Ba-O}$  and  $\text{Ba-N}_{\text{amine}}$  interatomic distances to the heteroatoms in the aza-crown-ether fragment are unremarkable and compare to those in the phenolato complex  $[\{\text{LO}\}\text{BaN}(\text{SiMe}_2\text{H})_2]$  (**3**) already mentioned.<sup>16</sup> Similarly, that  $\text{Ba-N}_{\text{silazide}}$  bond length in **5** ( $2.704(3)\text{ \AA}$ ) matches that in **3** ( $2.688(2)\text{ \AA}$ ). Coordination of the  $\text{N}_{\text{imine}}$  atom onto barium does not

induce a significant stretching of the C=N bond compared to that in the proligand (1.287(5) Å in **5** and 1.268(4) Å in the proligand). Complex **5** exhibits a mild Ba $\cdots$ H–Si anagostic interaction with H2<sub>si</sub>,<sup>18</sup> as indicated by the large discrepancy between the narrow Ba1–N4–Si2 and wider Ba1–N4–Si1 angles (104.90(14) and 126.02(16) °, respectively); this is consistent with the solution <sup>1</sup>H NMR data of the complex (see above). The barium atom protrudes greatly (1.76 Å) out of the mean plane formed by the atoms N2, C13, C14, C19 and N3. Note that there is a substantial distortion of the aromatic ring in the anilido fragment, and that the iminoanilido core made of these six carbons atoms together with C13, N2 and N3 deviates very clearly from the planarity observed in the proligand (Figure 3).

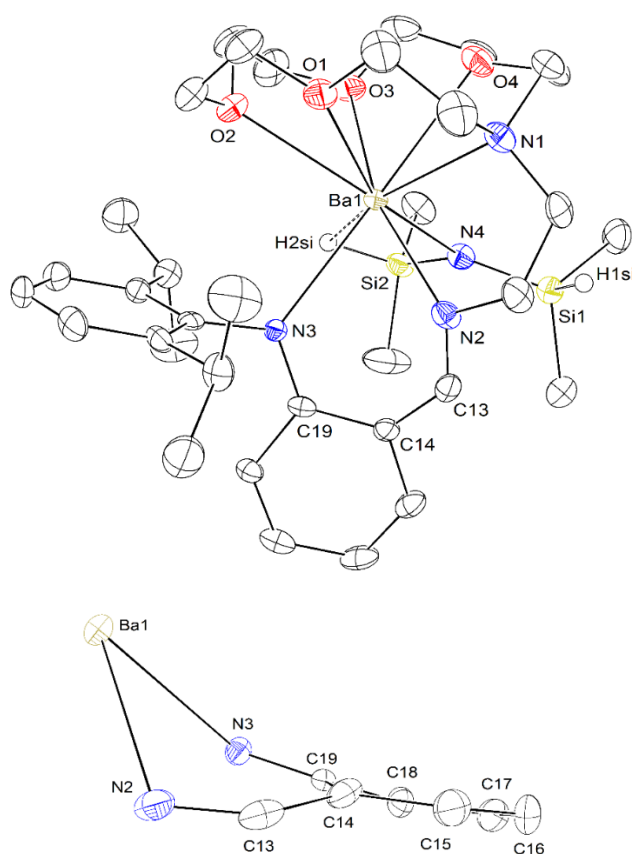


**Fig. 3.** Top, ORTEP representation of the molecular solid-state structure of [ $\{15\text{A}^{\text{crown}}\}\text{BaN}(\text{SiMe}_2\text{H})_2$ ] (**5**); bottom, representation of the non-planar iminoanilido core in the molecular solid-state structure of **5**. Ellipsoids at the 50% probability level. *CH* atoms omitted for clarity. Selected interatomic distances (Å) and angles (°): Ba1–N1 = 3.025(3), Ba1–N2 = 2.746(3), Ba1–N3 = 2.756(3), Ba1–N4 = 2.704(3), Ba1–O1 = 2.934(3), Ba1–O2 = 2.849(3), Ba1–O3 = 2.906(3), Ba1–O4 = 2.928(3), N2–C13 = 1.287(5), N2–C12 = 1.461(5); Si1–N4–Ba1 = 126.02(16), Si2–N4–Ba1 = 104.90(14).

The molecular structure of complex **6** is given in Figure 4; it shows one of the two distinct but very similar molecules of the complex found in the asymmetric unit. The final refinement ( $R_1 = 16.4\%$ ) for the structure is insufficient to enable a thorough discussion of the metric parameters, but the connectivity in the solid state could be established without ambiguity. The barium atom is seven-coordinate, with binding of all heteroatoms in the aza-crown-ether fragment completed by the nitrogen atom of tetramethylsilazide (N1) and, remarkably, by only one of the N atoms (N33) in the hence  $\eta^1$ -coordinated amidinate; the other N atom (N35) points away from the metal centre.

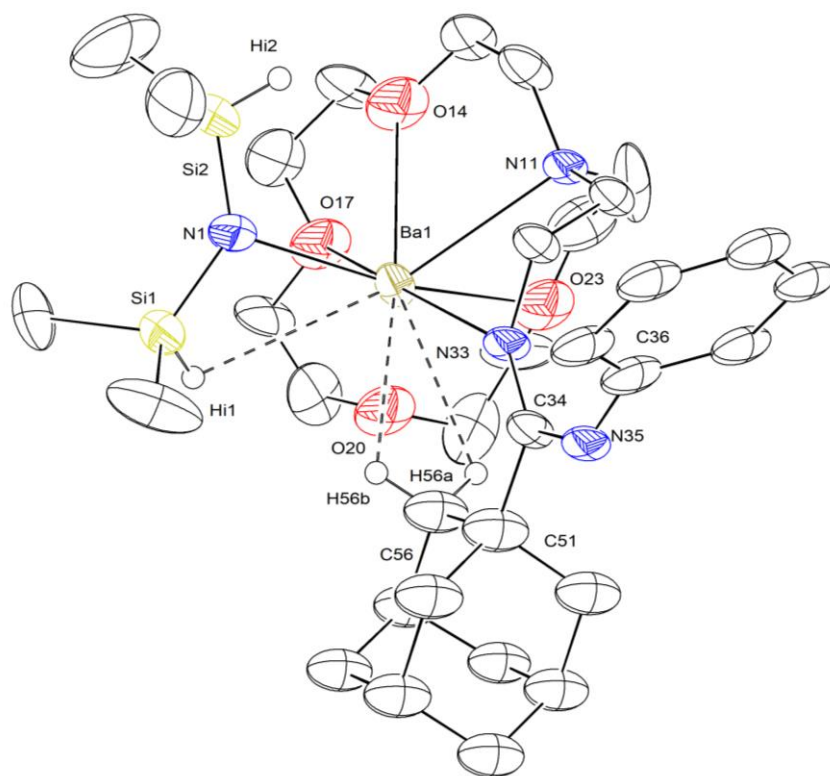


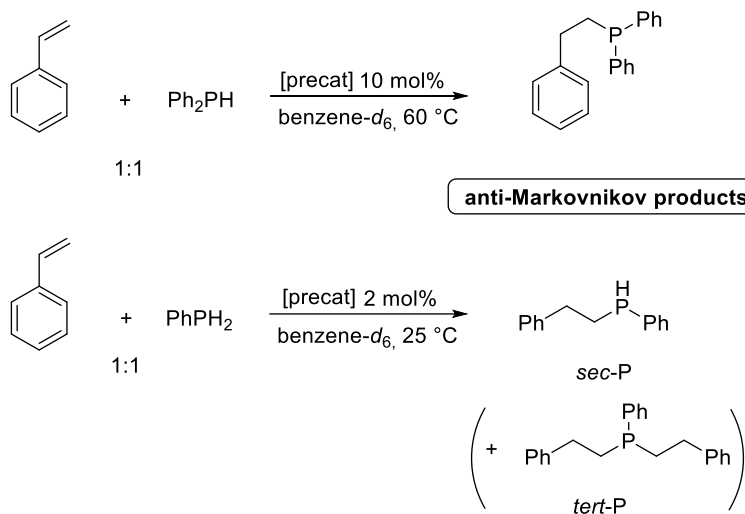
**Fig. 4.** ORTEP representation of the molecular solid-state structure of  $[\{Am^{crown}\}BaN(SiMe_2H)_2]$  (**6**). Only one of the two molecules in the asymmetric unit is represented. Ellipsoids at the 50% probability level. Non-interacting benzene molecules, *iPr* groups and H atoms other than those interactions with barium omitted for clarity. Poor refinement ( $R_1 = 16.4\%$ ) precludes a thorough discussion of metric parameters.

Note that counter-intuitively, the distance from the central carbon atom C34 to the metal-bound nitrogen atom N33 (ca. 1.33 Å) seems shorter than that to the non-coordinating one N35 (ca. 1.40 Å), but the poor refinement of the data set precludes a detailed analysis. The  $\eta^1$ -coordination mode observed for the amidinate in **6** is unusual. A similar one was observed in calcium-hydride amidinates, but these complexes featured an additional pattern of stabilising  $Ca \cdots C(\pi)$  interactions involving the flanking 2,6-*iPr*<sub>2</sub>C<sub>6</sub>H<sub>3</sub> substituents.<sup>12e</sup> There is no such interaction in **6**. On the other hand, the geometrical features of the

tetramethyldisilazide group, notably the largely different Ba1-N1-Si1 (ca. 106 °) and Ba1-N1-Si2 (ca. 120 °) angles, militate in favour of the presence of a Ba1⋯Hi1 β-Si–H anagostic interaction with Hi1.<sup>3,16,17,19</sup> Interestingly, the adamantyl substituent of the amidinate is directed towards the metal, and the short distances to the two hydrogen atoms H56a and H56b (ca. 2.80 Å) could indicate additional agostic bonding.

### *Barium-catalysed intermolecular hydrophosphination of vinylarenes*

The catalytic performances of [ $\{I^A^{crown}\}BaN(SiMe_2H)_2$ ] (**5**) and [ $\{Am^{crown}\}BaN(SiMe_2H)_2$ ] (**6**) in styrene hydrophosphination were examined in the light of earlier benchmark results obtained in our group for this catalysis.<sup>3d,5d</sup> Two reactions were initially examined (Scheme 3), involving the secondary phosphine HPPH<sub>2</sub> (the archetypal substrate in intermolecular hydrophosphination catalysis) and the primary phosphine PhPH<sub>2</sub>.



**Scheme 3.** Anti-Markovnikov hydrophosphination of styrene with HPPH<sub>2</sub> or PhPH<sub>2</sub> using [ $\{I^A^{crown}\}BaN(SiMe_2H)_2$ ] (**5**) as the pre-catalyst.

A preliminary assessment in the equimolar hydrophosphination of styrene with HPPH<sub>2</sub> (Scheme 3, top) showed that under otherwise identical experimental conditions ( $[styrene]_0/[HPPH_2]_0/[Ba]_0 = 10:10:1$ , benzene-*d*<sub>6</sub>, 60 °C, 60 min), complexes **5** (52% conversion, TOF = 0.5 h<sup>-1</sup>) and **6** (49% conversion, TOF = 0.5 h<sup>-1</sup>) both improve on the iminoanilide pre-catalyst [ $\{I^A^{Dipp^2}\}BaN(SiMe_3)_2.(thf)_2$ ] (32% conversion, TOF = 0.3 h<sup>-1</sup>) bearing two Dipp substituents reported previously by our group (Table 1).<sup>3c,3d</sup> In all cases, and characteristically for alkaline earth pre-catalysts,<sup>1</sup> the reactions are regioselective and only afford the anti-Markovnikov addition product PhCH<sub>2</sub>CH<sub>2</sub>PPh<sub>2</sub> ( $\delta_{31P} = -16.04$  ppm in benzene-*d*<sub>6</sub> at 60 °C); no trace of the branched product could be detected by NMR spectroscopy. Subsequent work focused on the somewhat more active and more soluble pre-catalyst **5**. Monitoring of the consumption of HPPH<sub>2</sub> during the reaction

catalysed by **5** showed that it is zeroth-order on the concentration [HPPh<sub>2</sub>]. This is reminiscent of the behaviour already known for [ $\{I^A^{Dipp2}\}BaN(SiMe_3)_2(thf)_2$ ], and for which the following kinetic rate law was established:<sup>3d</sup>

$$\text{rate} = k.[HPPh_2]^0.[\text{styrene}]^1.[Ba]^1 \quad (1)$$

It is therefore probable that in hydrophosphination reactions catalysed by **5**, the operative mechanism is identical to that with [ $\{I^A^{Dipp2}\}BaN(SiMe_3)_2(thf)_2$ ], with rate-limiting 2,1-insertion of the unsaturated C=C bond in the Ba–PPh<sub>2</sub> bond of a catalytically active [ $\{I^A^{Dipp2}\}BaPPh_2$ ] species (*vide infra*).

The rate of reactions catalysed by **5** increases substantially for reactions carried out without solvent. For instance, full conversion of 50 equivalents of HPPh<sub>2</sub> and styrene vs **5** was quantitative at 60 °C within 15 min, corresponding to a TOF value  $\geq 200 \text{ h}^{-1}$ . Complex **5** also mediates the regiospecific anti-Markovnikov hydrophosphination of styrene with PhPH<sub>2</sub> (Scheme 3, bottom). The conversion of 50 equivalents of styrene and phosphine ([styrene]<sub>0</sub>/[PhPH<sub>2</sub>]<sub>0</sub>/[**5**]<sub>0</sub> = 50:50:1) performed at 25 °C in benzene-*d*<sub>6</sub> is near-quantitative within 60 min. It yields the secondary phosphine PhPHCH<sub>2</sub>CH<sub>2</sub>Ph (doublet at  $\delta_{31P} = -52.41 \text{ ppm}$  in benzene-*d*<sub>6</sub> at 60 °C) with high selectivity, as only traces of the tertiary phosphine PhP(CH<sub>2</sub>CH<sub>2</sub>Ph)<sub>2</sub> (singlet at  $\delta_{31P} = -24.09 \text{ ppm}$ ) were detected by <sup>1</sup>H and <sup>31</sup>P NMR spectroscopy. The selectivity towards the secondary phosphine under these experimental conditions typically exceeds 95%. Note that under identical experimental conditions ([styrene]<sub>0</sub>/[PhPH<sub>2</sub>]<sub>0</sub>/[**5**]<sub>0</sub> = 50:50:1, 25 °C, 60 min, [metal]<sub>0</sub> = 11.5 mM in benzene-*d*<sub>6</sub>), the performance of **5** (93% conversion, TOF = 54 h<sup>-1</sup>) betters that displayed by the divalent rare-earth precatalysts [ $\{LO^{NO4}\}YbN(SiMe_3)_2$ ] (74% conversion, TOF = 37 h<sup>-1</sup>) and [ $\{LO^{NO4}\}SmN(SiMe_3)_2$ ] (63% conversion, TOF = 32 h<sup>-1</sup>) supported by the multidentate aminoether-phenolate  $\{LO^{NO4}\}^-$  (see Figure 1).<sup>5d</sup> Substrate conversion reaches near completion in the reaction of two equivalents of styrene vs PhPH<sub>2</sub> catalysed by **5** ([styrene]<sub>0</sub>/[PhPH<sub>2</sub>]<sub>0</sub>/[**5**]<sub>0</sub> = 50:25:1, 25 °C, 60 min, [**5**]<sub>0</sub> = 8.0 mM in benzene-*d*<sub>6</sub>), and the formation of the tertiary phosphine PhP(CH<sub>2</sub>CH<sub>2</sub>Ph)<sub>2</sub> is then selective.

**Table 1.** Comparative data for the hydrophosphination of styrene with HPPh<sub>2</sub> and various Ba precatalysts.

Precatalyst	[styrene] <sub>0</sub> /[HPPh <sub>2</sub> ] <sub>0</sub> /[Ba] <sub>0</sub>	Conversion <sup>b</sup> [%]	TOF <sup>c</sup> [h <sup>-1</sup> ]
[{I <sup>A</sup> crown}BaN(SiMe <sub>2</sub> H) <sub>2</sub> ] ( <b>5</b> )	10:10:1	52	0.52
[{Am <sup>crown</sup> }BaN(SiMe <sub>2</sub> H) <sub>2</sub> ] ( <b>6</b> )	10:10:1	49	0.49
[{I <sup>A</sup> Dipp <sup>2</sup> }BaN(SiMe <sub>3</sub> ) <sub>2</sub> .(thf) <sub>2</sub> ] <sup>d</sup>	10:10:1	32	0.32

<sup>a</sup> T = 60 °C, t = 60 min, benzene-*d*<sub>6</sub>, [Ba]<sub>0</sub> = 10 mM. <sup>b</sup> Conversion determined by <sup>1</sup>H NMR spectroscopy. <sup>c</sup> Turnover frequency. <sup>d</sup> See references 3c and 3d.

#### *On the nature of the active species in Ba-mediated intermolecular alkene hydrophosphination*

During the course of the hydrophosphination of styrene with HPPh<sub>2</sub> catalysed by **5** (see Scheme 3, top) carried out in benzene-*d*<sub>6</sub> at 60 °C, a small crop of orange single crystals formed out of solution. The identity of the compound, [{I<sup>A</sup> crown}BaPPh<sub>2</sub>] (**7**), was established by X-ray diffraction analysis.

The molecular structure of **7** shows the barium to rest in an eight-coordinate environment, with coordination of all heteroatoms from the macrocycle (Figure 5). To our knowledge, it is the first structurally authenticated heteroleptic barium-phosphide, although a number of homoleptic complexes have been previously reported, e.g. [{([Me<sub>3</sub>Si]<sub>2</sub>CH)(C<sub>6</sub>H<sub>3</sub>-2-OMe-3-Me)P}<sub>2</sub>Ba.(thf)<sub>2</sub>],<sup>20</sup> [Ba{P(SiMe<sub>3</sub>)<sub>2</sub>}<sub>2</sub>.(thf)<sub>4</sub>],<sup>21</sup> [Ba(PPh<sub>2</sub>)<sub>2</sub>.(thf)<sub>5</sub>],<sup>22</sup> and [Ba(PPh<sub>2</sub>)<sub>2</sub>.(18-crown-6)].<sup>23</sup> The Ba–N interatomic distances in **7** are commensurate with those measured in the parent amido complex **5**. The Ba–P bond length (3.3686(9) Å) is comparable to those in [Ba(PPh<sub>2</sub>)<sub>2</sub>.(thf)<sub>5</sub>] (3.328(2) and 3.345(2) Å) and [Ba(PPh<sub>2</sub>)<sub>2</sub>.(18-crown-6)] (3.3484(7) Å).<sup>22,23</sup>

The mononuclear complex **7** is thought to have formed under catalytic conditions upon deprotonation of the relatively acidic substrate HPPh<sub>2</sub> by precatalyst **5**, with concomitant release of HN(SiMe<sub>2</sub>H)<sub>2</sub>. An NMR scale reaction between **5** and a stoichiometric amount of HPPh<sub>2</sub> in thf-*d*<sub>8</sub> was consistent with the formation of a main new organometallic species assumed to be **7** (see ESI). Besides production of this new complex, the <sup>1</sup>H NMR spectrum indicated release of HN(SiMe<sub>2</sub>H)<sub>2</sub> and quantitative consumption of HPPh<sub>2</sub>, together with the presence a small amount, ca. 15%, of free {I<sup>A</sup> crown}H (presumably released through hydrolysis during sample preparation). The <sup>31</sup>P NMR spectrum confirmed full consumption of HPPh<sub>2</sub> (δ ca. –41 ppm),<sup>22</sup> and a broad resonance at ca. +5 ppm compatible with a putative [Ba]–PPh<sub>2</sub> species was detected.<sup>22-23</sup> Yet, the NMR data for the reaction between **5** and HPPh<sub>2</sub> also showed the presence of other unidentified species, and we failed to isolate analytically pure **7**. Catalytic studies with pre-isolated **7** could hence not be conducted. We therefore cannot assert with total confidence that **7**, which could not be isolated cleanly, is the sole active species under catalytic conditions.

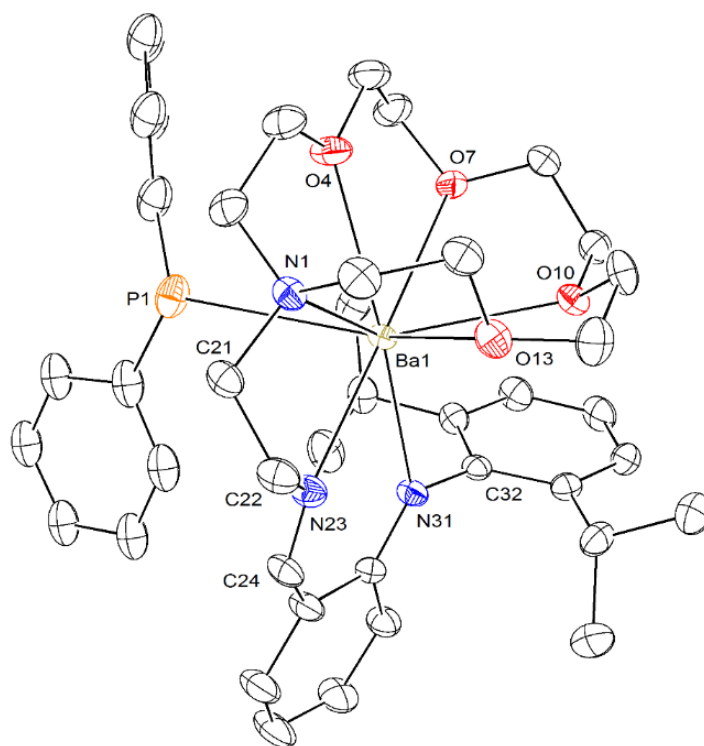
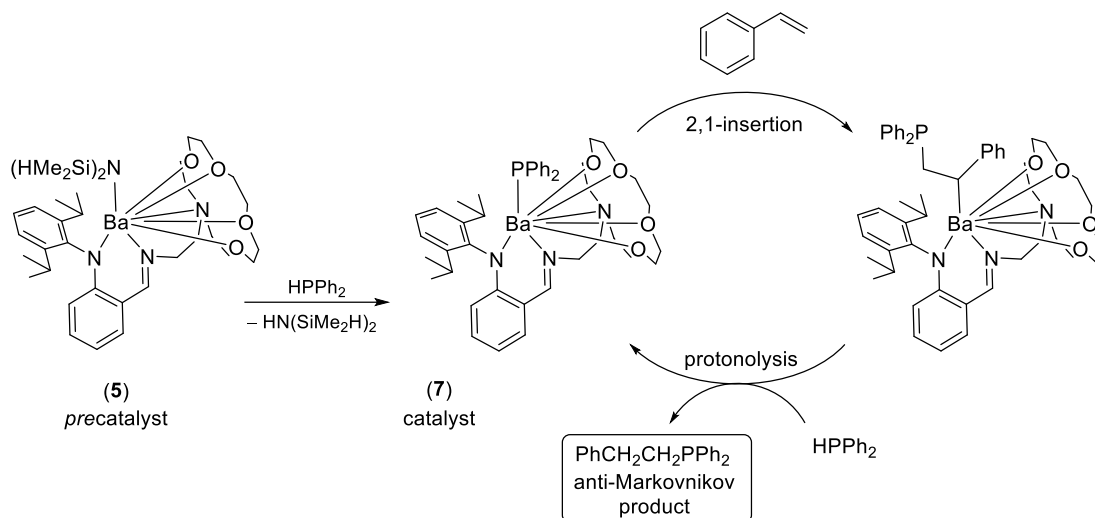


**Fig. 5.** ORTEP representation of the molecular solid-state structure of [ $\{15\text{Crown-5}\}\text{BaPPh}_2$ ] (**7**). Ellipsoids at the 50% probability level. H atoms and non-interacting benzene molecule omitted for clarity. One component of each disordered  $\text{C}_6\text{H}_5$  moieties is depicted. Selected interatomic distances ( $\text{\AA}$ ): Ba1-N31 = 2.691(2), Ba1-N23 = 2.780(2), Ba1-O10 = 2.847(2), Ba1-O4 = 2.869(2), Ba1-O7 = 2.886(2), Ba1-O13 = 2.886(2), Ba1-N1 = 2.972(2), Ba1-C32 = 3.302(3), Ba1-P1 = 3.3686(9).

Based on our earlier investigations of the mechanism of intermolecular hydrophosphination reactions,<sup>3d</sup> **7** is thought to be the catalytically active species in the catalysed hydrophosphination of styrene mediated by **5** (Scheme 4). Considering that the reactions only generate the anti-Markovnikov products of addition, the mechanism is proposed to involve 2,1-insertion of the polarised  $\text{Ph}(\text{H})\text{C}^{(\delta-)}=\text{C}^{(\delta+)}\text{H}_2$  double bond into the  $[\text{Ba}]\text{-PPh}_2$  bond in **7**, resulting in the production of a transient barium alkyl species  $[\text{Ba}]\text{-CH}(\text{Ph})\text{CH}_2\text{PPh}_2$ . This intermediate is then rapidly protonated by an incoming  $\text{HPPH}_2$  to release the product  $\text{PhCH}_2\text{CH}_2\text{PPh}_2$  and regenerate the active species **7**.



**Scheme 4.** Proposed mechanism for styrene/ $\text{HPPH}_2$  hydrophosphination catalysed by  $[(\text{IA}^{\text{crown}})\text{BaN}(\text{SiMe}_2\text{H})_2]$  (5).

## Conclusion

The two nitrogen-based proligands  $\{\text{IA}^{\text{crown}}\}\text{H}$  and  $\{\text{Am}^{\text{crown}}\}\text{H}$ , respectively an iminoaniline and an amidine bearing a tethered macrocycle side-arm prepared in multi-step procedures, enable the preparation of the heteroleptic barium complexes  $[(\text{IA}^{\text{crown}})\text{BaN}(\text{SiMe}_2\text{H})_2]$  and  $[(\text{Am}^{\text{crown}})\text{BaN}(\text{SiMe}_2\text{H})_2]$ . These solvent-free complexes have been characterised in the solid state, and they both exhibit high coordination numbers. The iminoanilide  $[(\text{IA}^{\text{crown}})\text{BaN}(\text{SiMe}_2\text{H})_2]$  mediates competently the hydrophosphination of styrene with primary and secondary phosphines. These reactions exhibit entire anti-Markovnikov selectivity, and they also generate chemoselectively a single secondary phosphine in the reaction of  $\text{PhPH}_2$  with either one or two equivalents of styrene.

## Conflicts of interest

There are no conflicts of interest to declare.

## Notes and references

‡ These two co-authors have contributed equally to the work.

# Note that the macrocyclic 1-aza-15-crown-5, i.e. the product of reaction (vi) in Scheme 1, is commercially available, but at prohibitive cost for large scale syntheses.

- 1 (a) S. Harder, *Chem. Rev.*, 2010, **110**, 3852; (b) M. R. Crimmin and M. S. Hill, *Top. Organomet. Chem.*, 2013, **45**, 191; (c) M. S. Hill, D. J. Liptrot and C. Weetman, *Chem. Soc. Rev.*, 2016, **45**, 972.
- 2 (a) M. R. Crimmin, I. J. Casely and M. S. Hill, *J. Am. Chem. Soc.*, 2005, **127**, 2042; (b) M. R. Crimmin, M. Arrowsmith, A. G. M. Barrett, I. J. Casely, M. S. Hill and P. A. Procopiu, *J. Am. Chem. Soc.*, 2009, **131**, 9670; (c) M. Arrowsmith, M. R. Crimmin, A. G. M. Barrett, M. S. Hill, G. Kociok-Köhn and P. A. Procopiu, *Organometallics*, 2011, **30**, 1493; (d) J. S. Wixey and B. D. Ward, *Chem. Commun.*, 2011, **47**, 5449; (e) B. Liu, T. Roisnel, J.-F. Carpentier and Y. Sarazin, *Chem. Eur. J.*, 2013, **19**, 2784; (f) N. Romero, S.-C. Roşca, Y. Sarazin, J.-F. Carpentier, L. Vendier, S. Mallet-Ladeira, C. Dinoi and M. Etienne, *Chem. Eur. J.*, 2015, **21**, 4115; (g) S. Tobisch, *Chem. Eur. J.*, 2015, **21**, 6765; (h) B. Freitag, C. A. Fischer, J. Penafiel, G. Ballmann, H. Elsen, C. Färber, D. F. Piesik and S. Harder, *Dalton Trans.*, 2017, **46**, 11192.
- 3 (a) A. G. M. Barrett, C. Brinkmann, M. R. Crimmin, M. S. Hill, P. Hunt and P. A. Procopiu, *J. Am. Chem. Soc.*, 2009, **131**, 12906; (b) C. Brinkmann, A. G. M. Barrett, M. S. Hill and P. A. Procopiu, *J. Am. Chem. Soc.*, 2012, **134**, 2193; (c) B. Liu, T. Roisnel, J.-F. Carpentier and Y. Sarazin, *Angew. Chem. Int. Ed.*, 2012, **51**, 4943; (d) B. Liu, T. Roisnel, J.-F. Carpentier and Y. Sarazin, *Chem. Eur. J.*, 2013, **19**, 13445; (e) S. Tobisch, *Chem. Eur. J.*, 2014, **20**, 8988.
- 4 (a) F. Buch, J. Brettar and S. Harder, *Angew. Chem. Int. Ed.*, 2006, **45**, 2741; (b) P. Jochmann, J. P. Davin, T. P. Spaniol, L. Maron and J. Okuda, *Angew. Chem. Int. Ed.*, 2012, **51**, 4452; (c) J. Intemann, H. Bauer, J. Pahl, L. Maron and S. Harder, *Chem. Eur. J.*, 2015, **21**, 11452.
- 5 See 2e, 3c, 3d and: (a) M. R. Crimmin, A. G. M. Barrett, M. S. Hill, P. B. Hitchcock and P. A. Procopiu, *Organometallics*, 2007, **26**, 2953; (b) H. Hu and C. Cui, *Organometallics*, 2012, **31**, 1208; (c) S.-C. Roşca, T. Roisnel, V. Dorcet, J.-F. Carpentier and Y. Sarazin, *Organometallics*, 2014, **33**, 5630; (d) I. V. Basalov, B. Liu, T. Roisnel, A. V. Cherkasov, G. K. Fukin, J.-F. Carpentier, Y. Sarazin and A. A. Trifonov, *Organometallics*, 2016, **35**, 3261; (e) B. J. Ward and P. A. Hunt, *ACS Catal.*, 2017, **7**, 459; (f) I. V. Lapshin, O. S. Yurova, I. V. Basalov, V. Yu. Rad'kov, E. I. Musina, A. V. Cherkasov,

- G. K. Fukin, A. A. Karasik and A. A. Trifonov, *Inorg. Chem.*, 2018, **57**, 2942; (g) I. V. Lapshin, I. V. Basalov, K. A. Lyssenko, A. V. Cherkasov and A. A. Trifonov, *Chem. Eur. J.*, 2019, **25**, 459.
- 6 (a) T. M. A. Al-Shboul, H. Görls and M. Westerhausen, *Inorg. Chem. Commun.*, 2008, **11**, 1419; (b) T. M. A. Al-Shboul, H. Görls, S. Krieck and M. Westerhausen, *Eur. J. Inorg. Chem.*, 2012, 5451; (c) F. M. Younis, S. Krieck, T. M. A. Al-Shboul, H. Görls and M. Westerhausen, *Inorg. Chem.*, 2016, **55**, 4676.
- 7 (a) M. S. Hill, D. J. Liptrot, D. J. MacDougall, M. F. Mahon and T. P. Robinson, *Chem. Sci.*, 2013, **4**, 4212; (b) C. Bellini, J.-F. Carpentier, S. Tobisch and Y. Sarazin, *Angew. Chem. Int. Ed.*, 2015, **54**, 7679.
- 8 O. I. Kolodiaznyi, *Top. Curr. Chem.*, 2015, **360**, 161.
- 9 D. Georgiadis and V. Dive, *Top. Curr. Chem.*, 2015, **360**, 1; (b) D. Virieux, J.-N. Volle, N. Bakalara and J.-L. Pirat, *Top. Curr. Chem.*, 2015, **360**, 39; (c) A. J. Wiemer and D. F. Wiemer, *Top. Curr. Chem.*, 2015, **360**, 115.
- 10 (a) Y. Sarazin, B. Liu, T. Roisnel, L. Maron and J.-F. Carpentier, *J. Am. Chem. Soc.*, 2011, **133**, 9069; (b) H. Bauer, M. Alonso, C. Fischer, B. Rösch, H. Elsen and S. Harder, *Angew. Chem. Int. Ed.*, 2018, **57**, 15177.
- 11 M. Arrowsmith, M. S. Hill and G. Kociok-Köhn, *Organometallics*, 2010, **29**, 4203.
- 12 (a) M. H. Chisholm, J. Gallucci and K. Phomphrai, *Chem. Commun.*, 2003, 48; (b) S. Datta, M.T. Gamer and P. W. Roesky, *Organometallics*, 2008, **27**, 1207; (c) T. D. Nixon and B. D. Ward, *Chem. Commun.*, 2012, **48**, 11790; (d) M. Arrowsmith, M. S. Hill and G. Kociok-Köhn, *Organometallics*, 2014, **33**, 206; (e) A. Causero, G. Ballmann, J. Pahl, H. Zijlstra, C. Färber and S. Harder, *Organometallics*, 2016, **35**, 3350; (f) X. Shi, C. Hou, C. Zhou, Y. Song and J. Cheng, *Angew. Chem. Int. Ed.*, 2017, **56**, 16650.
- 13 (a) S. Harder and J. Brettar, *Angew. Chem. Int. Ed.*, 2006, **45**, 3474; (b) C. Ruspic, S. Nembenna, A. Hofmeister, J. Magull, S. Harder and H. W. Roesky, *J. Am. Chem. Soc.*, 2006, **128**, 15000; (c) C. Ruspic and S. Harder, *Inorg. Chem.*, 2007, **46**, 10426; (d) S. Nembenna, H. W. Roesky, S. Nagendran, A. Hofmeister, J. Magull, P.-J. Wilbrandt and M. Hahn, *Angew. Chem. Int. Ed.*, 2007, **46**, 2512; (e) A. S. S. Wilson, M. S. Hill, M. F. Mahon, C. Dinoi and L. Maron, *Science*, 2017, **358**, 1168.
- 14 (a) A. Causero, H. Elsen, G. Ballmann, A. Escalona and S. Harder, *Chem. Commun.*, 2017, **53**, 10386; (b) B. Freitag, J. Pahl, C. Färber and S. Harder, *Organometallics*, 2018, **37**, 469; (c) C. N. de Bruin-Dickason, T. Sutcliffe, C. Alvarez Lamsfus, G. B. Deacon, L. Maron and C. Jones, *Chem. Commun.*, 2018, **54**, 786.
- 15 (a) V. Leich, T. P. Spaniol, L. Maron and J. Okuda, *Angew. Chem. Int. Ed.*, 2016, **55**, 4794; (b) D. Schuhknecht, C. Lhotzky, T. P. Spaniol, L. Maron and J. Okuda, *Angew. Chem. Int. Ed.*, 2017, **56**,

- 12367; (c) M. Wiesinger, B. Maitland, C. Färber, G. Ballmann, C. Fischer, H. Elsen and S. Harder, *Angew. Chem. Int. Ed.*, 2017, **56**, 16654.
- 16 Y. Sarazin, D. Roşca, V. Poirier, T. Roisnel, A. Silvestru, L. Maron and J.-F. Carpentier, *Organometallics*, 2010, **29**, 6569.
- 17 O. Michel, S. König, K. W. Törnroos, C. Maichle-Mössmer and R. Anwander, *Chem. Eur. J.*, 2011, **17**, 11857.
- 18 H1<sub>Si</sub> and H2<sub>Si</sub> hydrogen atoms linked to silicon atoms were introduced in the structural model through Fourier difference maps analysis.
- 19 (a) O. Michel, K. W. Törnroos, C. Maichle-Mössmer and R. Anwander, *Chem. Eur. J.*, 2011, **17**, 4964; (b) O. Michel, K. W. Törnroos, C. Maichle-Mössmer and R. Anwander, *Eur. J. Inorg. Chem.*, 2012, 44; (c) B. Liu, T. Roisnel, J.-P. Guégan, J.-F. Carpentier and Y. Sarazin, *Chem. Eur. J.*, 2012, **18**, 6289; (d) J. P. Davin, J.-C. Buffet, T. P. Spaniol and J. Okuda, *Dalton Trans.*, 2012, **41**, 12612; (e) S.-C. Roşca, C. Dinoi, E. Caytan, V. Dorcet, M. Etienne, J.-F. Carpentier and Y. Sarazin, *Chem. Eur. J.*, 2016, **22**, 6505; (f) S.-C. Roşca, E. Caytan, V. Dorcet, T. Roisnel, J.-F. Carpentier and Y. Sarazin, *Organometallics*, 2017, **36**, 1269; (g) D. Mukherjee, S. Shirase, K. Beckerle, T. P. Spaniol, K. Mashima and J. Okuda, *Dalton Trans.*, 2017, **46**, 8451; (h) E. Le Coz, H. Roueindeji, V. Dorcet, T. Roisnel, J.-F. Carpentier and Y. Sarazin, *Dalton Trans.*, **2019**, DOI: 10.1039/C9DT00771G.
- 20 S. Blair, K. Izod, W. Clegg and R. W. Harrington, *Inorg. Chem.*, 2004, **43**, 8526.
- 21 M. Westerhausen and W. Schwarz, *J. Organomet. Chem.*, 1993, **463**, 51.
- 22 M. Gärtner, H. Görls and M. Westerhausen, *Z. Anorg. Allg. Chem.*, 2007, **633**, 2025.
- 23 M. R. Crimmin, A. G. M. Barrett, M. S. Hill, P. B. Hitchcock and P. A. Procopiu, *Inorg. Chem.*, 2007, **46**, 10410.